

Viscosity in cosmological simulations of clusters of galaxies

Marcus Brüggen¹, Mateusz Ruszkowski^{2,3}

ABSTRACT

The physics of the intracluster medium, in particular the values for the thermal conductivity and the viscosity are largely unknown and subject to an ongoing debate. Here, we study the effect of viscosity on the thermal state of the intracluster medium using three-dimensional cosmological simulations of structure formation. It is shown that viscosity, provided it is not too far off from the unmagnetised Spitzer value, has a significant effect on cluster profiles. In particular, it aids in heating the cool cores of clusters. The central cooling time of the most massive clusters in our simulation is increased by more than an order of magnitude. In large clusters, viscous heating may help to establish an entropy floor and to prevent a cooling catastrophe.

Subject headings: galaxies: active - galaxies: clusters: cooling flows - X-rays: galaxies

1. Introduction

Cooling by bremsstrahlung and line emission leads to a loss of pressure support in the centers of galaxy clusters, which, in the absence of non-gravitational heating, would cause a slow, subsonic inflow of gas towards the center of the gravitational well. As a result, cluster cores should cool and accrete gas at rates of hundreds and more solar masses per year. This scenario is in conflict with observational evidence that indicates that mass deposition rates are consistently lower than predicted. Moreover, the gas temperatures in cluster centers are maintained typically above ~ 2 keV (Peterson et al. 2001).

More evidence for non-gravitational heating in clusters comes from cluster scaling relations. These relations show departures from self-similarity: In the absence of non-gravitational

¹International University Bremen, Campus Ring 1, 28759 Bremen, Germany

²JILA, Campus Box 440, University of Colorado at Boulder, CO 80309-0440

³*Chandra* Fellow

heating and radiative cooling, the entropy is expected to scale linearly with the mean cluster temperature. However, observations by Ponman, Sanderson & Finoguenov (2003), Pratt & Arnaud (2005) and Piffaretti et al. (2005) indicate a scaling of entropy roughly according to $T^{2/3}$. Moreover, they reveal a systematic excess of entropy in low-mass clusters (e.g., Ponman, Sanderson & Finoguenov 2003). Churazov et al. (2001); Brüggen et al. (2002); Brüggen & Kaiser (2002) have argued that heating by a central AGN can keep the ICM from cooling dramatically in the center.

Thermal conduction has been put forward to explain the absence of soft X-rays from galaxy clusters (Kim & Narayan (2003) and references therein). Cosmological simulations with thermal conduction have been performed by Dolag et al. (2004) and Jubelgas et al. (2004). If thermal conduction is at work, other transport processes such as viscosity are bound to be important, too. Thermal conduction transports energy and is mediated mainly by the faster electrons. Viscosity, on the other hand, transports momentum and is mediated primarily by the more massive ions. It is not clear that the suppression factors of both transport processes should be the same. Whether they are the same may depend on the scale magnetic fluctuations extend to. This scale may be much larger than the gyroradii of electrons and ions (in which case suppression factors could be comparable) or it could be comparable to the ion gyroradius. The magnitude of the suppression factor is motivated by various theoretical arguments (e.g., given in Narayan & Medvedev 2001). However, we note that the precise value of the suppression factor is highly uncertain and, depending on the nature of magnetic turbulence, may even exceed the Spitzer value (Cho et al. 2003) or be suppressed well below it.

Based on observations of the Perseus cluster, it has been suggested by Fabian et al. (2003) that viscosity may play an important role in dissipating energy injected by the central AGN. The case for this is based on the existence of long, straight H α -filaments that appear to rule out the presence of strong turbulence in the cores of galaxy clusters. The Reynolds number for a fluid flow whose viscosity is suppressed with a factor, f , with respect to the Spitzer value, is given by

$$\text{Re} \sim 50 f_{0.3}^{-1} n_{e,-3} L_{\text{kpc}} v_{500} T_7^{-5/2}, \quad (1)$$

where $n_{e,-3}$ is the electron number density in units of 10^{-3} cm^{-3} , L_{kpc} the typical size of an eddy in units of kpc, v_{500} the associated velocity in units of 500 km s^{-1} and T_7 the temperature of the fluid in 10^7 K . As such values of Reynolds numbers are below the critical value that separates laminar and turbulent regimes, it was concluded that viscosity can play an

appreciable role in the ICM, provided that viscosity is not heavily suppressed.

Subsequently, heating by viscous dissipation of AGN-induced motions has been simulated by Ruszkowski et al. (2004a,b); Brügggen et al. (2005). It was concluded that, provided viscosity is not suppressed significantly with respect to its unmagnetised value, viscous dissipation of AGN-induced motions can balance the radiative losses in the ICM. In Reynolds et al. (2005) the effect of viscosity on the evolution of radio bubbles was studied, and it was found that viscosity had a stabilising effect on underdense bubbles. Fujita et al. (2004) have studied the dissipation of motions induced by acoustic-gravity waves in cluster cores. They find that, provided the wave amplitude is large enough, they can suppress the radiative cooling of the cores. Kim et al. (2005) have investigated the heating of clusters by dynamical friction. They concluded that friction can be an important supplier of heat but is unlikely to prevent the onset of cooling flows.

Meanwhile, cosmological simulations of galaxy clusters with, both, particle and grid-based methods have reached a fairly mature state. In particular, the addition of increasingly sophisticated recipes for radiative losses, star formation and stellar feedback have led to cluster models that can produce many observed features of galaxy clusters (Loken et al. 2002).

Motl et al. (2004) have simulated the formation of cool cores and observed that any “cooling flow” is overwhelmed by the velocity field inside the cluster, which has speeds of up to 2000 km s^{-1} . Nonetheless, such violent motions did not prevent the formation of cool cores. This shows that the formation of cool cores is inevitable unless some source of heating is present. Full 3D cluster collision simulations by Ritchie & Thomas (2002) and Ricker & Sarazin (2001) show that mergers can disrupt cooling flows. It is a common feature of all cosmological simulations of galaxy clusters that the ICM shows a substantial velocity field with many motions being supersonic. The ICM shows a complex dynamics with cool fronts, filaments, shocks etc. New observations confirm this picture. Detailed observations of unprecedented resolution by the latest X-ray observatories have revealed a rich portfolio of substructure in galaxy clusters. For example, Schuecker et al. (2001) find substructure in the majority of clusters in their REFLEX+BCS cluster sample. The ubiquity of substructure points to a high frequency of mergers and other events that prevent the cluster from relaxing to a smooth, unperturbed state.

Both, observations and simulations suggest that the ICM is in violent motion and that relaxed clusters, in which the gas sits almost statically in its potential well, are very rare, if

they exist at all. In the presence of viscosity, a fraction of the kinetic energy in these motions can be dissipated to heat the ICM. Thus, even in inactive phases of a central AGN, there can be heating in the form of viscous dissipation.

In this paper, we study the effect of viscosity on the intracluster medium in a cosmological simulation. In particular, we wish to compute to what extent viscous dissipation of random motions in a cluster can contribute to the heating of cluster cores. In the next section, we describe the technique and setup of our simulations. Finally, the results are discussed in Sec. 3.

2. Simulation

The simulations were performed with the hydrodynamics code Enzo developed by Bryan & Norman (1997) and Norman & Bryan (1999). Enzo is a grid-based hybrid code that couples N-body computations with Eulerian hydrodynamics. It is parallelised using the MPI (Message Passing Interface) library, and is designed to perform simulations of cosmological structure formation. In Enzo, the resolution of the equations is adaptive in, both, time and space. In space, more finely resolved child grids are produced where user-specified refinement criteria are met. In our simulations, each child grid has a factor 2 higher spatial resolution than its parent grid and a factor 8 higher mass resolution. For our purposes, the refinement is controlled by the overdensity of dark matter and baryons, as well as the temperature. In our setting, every cell whose overdensity was higher than 4 and had a temperature above 10^6 K was flagged for refinement. All cells on a given level are advanced with the same time step.

Enzo uses a particle-mesh N-body method to calculate collisionless particle dynamics. The dark matter particles are distributed onto the grids using cloud-in-cell interpolation. The gravitational potential is calculated on a periodic root grid using Fast Fourier Transforms. To calculate the potential on the more finely resolved subgrids, a multigrid relaxation method is used. Forces are computed on the mesh by finite differences, and then interpolated onto particle positions.

In our simulations, we included radiative cooling, assuming that all species in the baryonic gas are in equilibrium. The cooling was calculated from a tabulated cooling curve (Westbury & Henriksen 1992) for a plasma of fixed 0.3 solar abundance. The cooling curve is truncated at a minimum temperature of 10^4 K.

We used a star formation model by Cen & Ostriker (1992). According to this recipe, gas

is converted into collisionless star particles in regions that are Jeans unstable, contracting ($\nabla \cdot v < 0$) and cooling rapidly. If these three conditions are met inside a computational cell, a fraction of the cell’s baryonic mass is converted into a collisionless particle.

In O’Shea et al. (2005), Enzo was compared to SPH simulations using the GADGET code. General agreement in the distributions of temperature, entropy and density within clusters was found between both numerical methods.

Our simulations have a comoving box size of 64 Mpc/ h . We chose a standard flat Λ CDM cosmology with $\Omega_b = 0.044$, $\Omega_m = 0.27$, $\Omega_\Lambda = 0.73$, $h = 0.71$ and $\sigma_8 = 0.9$. We started from initial conditions at a redshift of $z_{\text{init}} = 60$. With 8 levels of refinement and a root grid of 64^3 cells, we achieve an effective resolution of 3.9 kpc/ h . The simulations were run on 32 processor of an IBM p690 shared-memory machine.

The evolution of internal energy is followed by solving the energy equation

$$\frac{\partial(\rho\epsilon)}{\partial t} + \nabla \cdot (\rho\epsilon + p)\mathbf{v} = \rho\mathbf{v} \cdot \mathbf{g} + \rho\dot{\epsilon}_{\text{visc}}, \quad (2)$$

where ϵ is energy per unit mass, ρ density, \mathbf{v} velocity and p pressure. The dissipation of mechanical energy due to viscosity, per unit mass of the fluid, is given by (Batchelor 1967, Shu 1992, Landau & Lifshitz 1997)

$$\dot{\epsilon}_{\text{visc}} = \frac{2\mu}{\rho} \left(e_{ij}e_{ij} - \frac{1}{3}\Delta^2 \right), \quad (3)$$

where $\Delta = e_{ii}$ and

$$e_{ij} = \frac{1}{2} \left(\frac{\partial v_i}{\partial x_j} + \frac{\partial v_j}{\partial x_i} \right), \quad (4)$$

and where μ is the dynamical coefficient of viscosity. In our simulations with viscosity, we use a third of the standard Spitzer viscosity for an unmagnetized plasma (Spitzer 1962), which is $\mu = 6.0 \times 10^{-17} T^{5/2} \text{ g cm}^{-1} \text{ s}^{-1}$, taking the Coulomb logarithm to be $\ln \Lambda = 37$. For simplicity and want for any better model, we assumed that μ is constant over cosmic time. This is a simplification that is unlikely to be strictly true because magnetic fields that inhibit viscosity will only be generated as structures evolve in the universe. It is not clear when and how magnetic fields form (see, e.g., Brügggen et al. (2005)). However, at early

times, certainly at redshifts higher than 3, viscous heating is relatively unimportant because the temperatures are quite small. Consequently, it appears unlikely that this simplification will affect our conclusions.

The timestep was modified to be the smaller value of the viscous and the Courant time step, i.e.:

$$dt = \min(dt_{\text{Cour}}, dt_{\text{visc}}) , \quad (5)$$

where dt_{Cour} is the Courant time step and $dt_{\text{visc}} = 0.1\min(dx_i^2/\mu)$.

Velocity diffusion was simulated by solving the momentum equation

$$\frac{\partial(\rho v_i)}{\partial t} + \frac{\partial}{\partial x_k}(\rho v_k v_i) + \frac{\partial P}{\partial x_i} = \rho g_i + \frac{\partial \pi_{ik}}{\partial x_k}, \quad (6)$$

where

$$\pi_{ik} = \frac{\partial}{\partial x_k} \left[2\mu \left(e_{ik} - \frac{1}{3}\Delta\delta_{ik} \right) \right] \quad (7)$$

and all other symbols have their usual meaning.

3. Results and discussion

We produced two simulations: one without viscosity and one with a third of Spitzer viscosity. Both runs included radiative cooling and star formation. A density projection of the viscous simulation is shown in Fig. 1. The largest cluster is situated near the upper edge of this figure.

Halos were identified using the HOP-algorithm developed by Eisenstein & Hut (1997). The parameters of the most massive cluster in our simulation are summarised in table 1. The virial radius is calculated for an overdensity of $\delta\rho/\rho = 200$, and the virial mass is the total mass (dark matter + baryons) within the virial radius. L_X is the total X-ray luminosity within R_{vir} in the band from 0.1 - 2.4 keV. Finally, M_{stars} is the total mass converted to stars. It is striking that, while the gross features of the cluster, such as virial radius, mass and temperature, are nearly identical between the runs, the X-ray luminosities differ

substantially. The X-ray luminosity depends on the density squared and is thus dominated by the central portion of the clusters. As discussed in the next section, there are pronounced differences in the central densities, which do not affect the total mass, though. Also, the mass converted to stars differ between the two runs, with the viscous run producing less stars.

In Fig. 2 - 5 we show the mass-weighted temperature, density, cooling time and entropy, respectively, as a function of radius in the most massive, non-merging cluster in our sample. While a cool core forms in the run without viscosity, it is absent in the viscous run. As can be seen from the temperature profile, Fig. 2, viscosity has essentially removed the cool core and the mass-weighted temperature even rises slightly in the centre. The density profiles also show significant differences (see Fig. 3). In the presence of viscosity, the density is nearly constant in the core, whereas, in the non-viscous run, it rises sharply in the inner 40 kpc. With 1/3 Spitzer viscosity, the density is very flat over the inner hundred kiloparsecs. In summary, we find that the runs with viscous dissipation lead to a hotter and less dense core. Consequently, the cooling time increases in the center, with respect to the non-viscous runs (see Fig. 4). The central cooling time is about two orders of magnitude higher than in the non-viscous case and larger than the Hubble time. If viscous heating was this efficient, no other sources of heating would be required to prevent a cooling catastrophe. The entropy, which is shown in Fig. 5, displays a very extended floor and has no central dip as in the run without viscosity. A comparison of a statistically relevant sample of simulated clusters can be compared with observed samples, such as the one by Donahue et al. (2005). Thus, one may be able to constrain the viscosity of the ICM from X-ray observations.

In Fig. 6 we compare the X-ray luminosity from the cluster in the band from 0.1 - 2.4 keV. In the case with viscosity, it is apparent that the cluster is more extended and that it lacks a strong emission spike in the center.

Table 1. Properties of the most massive cluster in our sample

	without visc	with visc
R_{virial}	1.11 Mpc	1.12 Mpc
M_{virial}	$2.2 \times 10^{14} M_{\odot}$	$2.3 \times 10^{14} M_{\odot}$
L_{x}	$1.6 \times 10^{46} \text{ erg s}^{-1}$	$2.2 \times 10^{45} \text{ erg s}^{-1}$
T_{vir}	$3.0 \times 10^7 \text{ K}$	$3.1 \times 10^7 \text{ K}$
M_{stars}	$7.4 \times 10^{12} M_{\odot}$	$6.5 \times 10^{12} M_{\odot}$

The temperature-dependence of viscosity biases this mode of heating towards hotter, more massive clusters, and will, thus, affect cluster scaling relations. We find that the effect of viscosity becomes systematically less important with decreasing mass of the cluster. In Fig. 7 - Fig. 9, we show the corresponding profiles of a smaller cluster with a mass of $9.7 \times 10^{13} M_{\odot}$. Evidently, viscosity only has a minor effect on the central density profile. A proper study of this effect requires a bigger simulation box that contains a large number of clusters, and is the subject of future work.

Note that in the simulations presented here, heat conduction has been neglected. As argued above, heat conduction and viscosity are intrinsically linked, and it would be interesting to study their joint effect on the cluster. Since the suppression factors of viscosity and conductivity are unknown, the consideration of heat conduction introduces another, essentially free, parameter into the problem. For this first simulation, we decided to study the isolated effect of viscosity only.

In order to validate our code modules, we have repeated a low-level test simulation in a small box with the FLASH code. The viscosity routines in FLASH have been tested in Ruszkowski et al. (2004a,b). Starting from similar initial conditions and including the same physics, we obtain very similar results between Enzo and FLASH.

As a result of numerical diffusion, the effective Reynolds number will be finite, even in the zero-viscosity case. The effective Reynolds numbers attainable in the simulation are proportional to the number of grid points across the fluctuation of interest to the power n , where $n = 3$ is the order of the numerical scheme¹ (Porter & Woodward 1994). As expressed in Eq. 1, the Reynolds number in the ICM is of the order of 50, assuming 0.3 of the Spitzer value. Test simulations with FLASH and Enzo suggest that the effective Reynolds number for the resolution chosen here is > 1000 . Both runs that we have presented here have identical spatial resolution. Hence, the differences between the runs are solely due to the physical viscosity.

Both, radiative losses and viscosity, are sensitive to the spatial resolution of the computational grid. We experimented with different refinement criteria and compared results from runs with different effective resolutions. Generally, the effect of physical viscosity becomes larger as the resolution increases. The same is true for radiative losses. The results pre-

¹See, e.g., Bowers & Wilson (1991) for the definition of “the order of the numerical scheme”, as it is different from the customary definition of accuracy of a perturbative calculation.

sented here seem to be reasonably converged and differ only marginally from the run with a refinement level less.

Assuming hydrostatic equilibrium when inferring cluster masses from synthetic observations, leads to masses that are systematically lower (by 10-15 per cent) than the actual cluster masses in simulations. This affects cluster constraints on cosmological parameters (see e.g., Allen et al. (2004)). If the ICM is viscous, it is conceivable that the assumption of hydrostatic equilibrium is better met. Thus, gas viscosity may reduce systematic deviations of cluster masses inferred from X-ray observations from their true values, which, in turn, may have consequences for precision measurements of cosmological parameters.

4. Summary

In a simple numerical experiment, we added physical viscosity to a cosmological simulation and studied its effect on cluster properties. The results of this experiment are interesting.

A viscosity not too far off from the unmagnetised Spitzer value can alleviate the problem of cool cores in galaxy clusters. Viscosity raises the temperature in the core and reduces the central cooling times significantly. This effect is important for massive clusters, but becomes ineffective for smaller clusters and groups. For 1/3 of Spitzer viscosity, the effect is important for cluster above $\sim 10^{14} M_{\odot}$. Feedback from star and AGN has been ignored in this work. These are additional sources of heat that will increase viscous heating. The interplay of various feedback processes with a possibly viscous ICM may complicate matters and should be looked at in future work.

As discussed above, the actual value of the viscosity in the ICM is subject to speculation, and the viscosity is essentially a free parameter. Here, we assumed that the magnetic field is not too efficient in suppressing viscosity and took a fiducial value of a third of Spitzer viscosity. Value cited in various studies in the recent literature assume value between 1/3 and 1/10 of the Spitzer value. Only if magnetic fields should suppress the viscosity by 2 orders of magnitude or more, the effect will start to be negligible. We defer the study of the effects of viscosity on the statistical properties of clusters and groups to a future publication based on a bigger simulation box containing a large number of clusters.

Real clusters may possess complex magnetic field configurations that lead to a very

inhomogeneous and anisotropic viscosity. This, in turn, can lead to complex dynamics of the ICM. It will be a challenge for future work to disentangle the effects of transport processes and magnetic fields.

We thank Brian O’Shea for providing us with non-public modules of Enzo and for valuable help. Eric Hallman is thanked for insightful discussions. M.B. acknowledges support by DFG grant BR 2026/3 within the Priority Programme ‘Witnesses of Cosmic History’ and the supercomputing grant NIC 1658 at the John-Neumann Institut at the Forschungszentrum Jülich. M.R. acknowledges support from NSF grant AST 03-07502 and NASA through Chandra Fellowship award PF3-40029 issued by the *Chandra X-Ray Observatory* Center, which is operated by the Smithsonian Astrophysical Observatory for and on behalf of NASA under contract NAS8-39073.

REFERENCES

- Allen, S. W., Schmidt, R. W., Ebeling, H., Fabian, A. C., & van Speybroeck, L. 2004, *MNRAS*, 353, 457
- Bowers, R. L. & Wilson, J. R. 1991, *Numerical modeling in applied physics and astrophysics* (Boston : Jones and Bartlett, c1991.)
- Brüggen, M. & Kaiser, C. R. 2002, *Nature*, 418, 301
- Brüggen, M., Kaiser, C. R., Churazov, E., & Enßlin, T. A. 2002, *MNRAS*, 331, 545
- Brüggen, M., Ruszkowski, M., & Hallman, E. 2005, *ApJ*, 630, 740
- Bryan, G. L. & Norman, M. L. 1997, in *ASP Conf. Ser. 123: Computational Astrophysics; 12th Kingston Meeting on Theoretical Astrophysics*, 363–+
- Cen, R. & Ostriker, J. P. 1992, *ApJ*, 399, L113
- Cho, J., Lazarian, A., Honein, A., Knaepen, B., Kassinos, S., & Moin, P. 2003, *ApJ*, 589, L77
- Churazov, E., Brüggen, M., Kaiser, C. R., Böhringer, H., & Forman, W. 2001, *ApJ*, 554, 261
- Dolag, K., Jubelgas, M., Springel, V., Borgani, S., & Rasia, E. 2004, *ApJ*, 606, L97
- Donahue, M. and Horner, D. J., Cavagnolo, K. W., & Voit, G. 2005, *ArXiv Astrophysics e-prints*, astro-ph/0511401
- Eisenstein & Hut, P. 1997, *astro-ph/9712200*, 1, 1
- Fabian, A. C., Sanders, J. S., Allen, S. W., Crawford, C. S., Iwasawa, K., Johnstone, R. M., Schmidt, R. W., & Taylor, G. B. 2003, *MNRAS*, 344, L43
- Fujita, Y., Matsumoto, T., & Wada, K. 2004, *ApJ*, 612, L9
- Jubelgas, M., Springel, V., & Dolag, K. 2004, *MNRAS*, 351, 423
- Kim, W.-T., El-Zant, A. A., & Kamionkowski, M. 2005, *ApJ*, 632, 157
- Kim, W.-T. & Narayan, R. 2003, *ApJ*, 596, 889
- Loken, C., Norman, M. L., Nelson, E., Burns, J., Bryan, G. L., & Motl, P. 2002, *ApJ*, 579, 571

- Motl, P. M., Burns, J. O., Loken, C., Norman, M. L., & Bryan, G. 2004, *ApJ*, 606, 635
- Narayan, R. & Medvedev, M. V. 2001, *ApJ*, 562, L129
- Norman, M. L. & Bryan, G. L. 1999, in *ASSL Vol. 240: Numerical Astrophysics*, 19–+
- O’Shea, B. W., Nagamine, K., Springel, V., Hernquist, L., & Norman, M. L. 2005, *ApJS*, 160, 1
- Peterson, J. R., Paerels, F. B. S., Kaastra, J. S., Arnaud, M., Reiprich, T. H., Fabian, A. C., Mushotzky, R. F., Jernigan, J. G., & Sakelliou, I. 2001, *A&A*, 365, L104
- Porter, D. H. & Woodward, P. R. 1994, *ApJS*, 93, 309
- Reynolds, C. S., McKernan, B., Fabian, A. C., Stone, J. M., & Vernaleo, J. C. 2005, *MNRAS*, 357, 242
- Ricker, P. M. & Sarazin, C. L. 2001, *ApJ*, 561, 621
- Ritchie, B. W. & Thomas, P. A. 2002, *MNRAS*, 329, 675
- Ruszkowski, M., Brüggén, M., & Begelman, M. C. 2004a, *ApJ*, 611, 158
- . 2004b, *ApJ*, 615, 675
- Schuecker, P., Böhringer, H., Reiprich, T. H., & Feretti, L. 2001, *A&A*, 378, 408
- Spitzer, L. 1962, *Physics of Fully Ionized Gases (Physics of Fully Ionized Gases, New York: Interscience (2nd edition), 1962)*
- Westbury, C. F. & Henriksen, R. N. 1992, *ApJ*, 388, 64

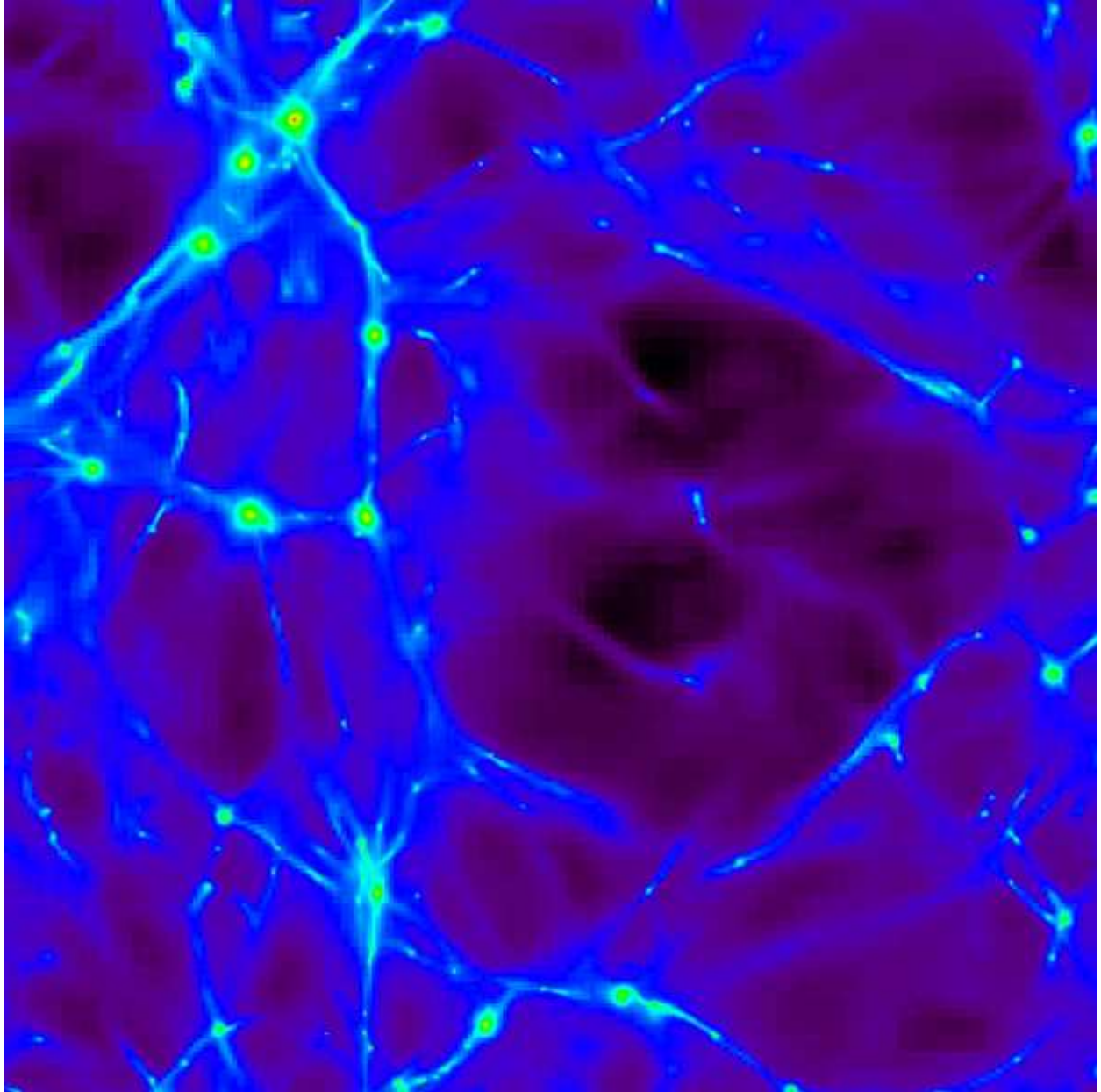


Fig. 1.— Projected gas density at $z = 0.25$ showing the most massive cluster in the simulation volume. The side length in this figure is $60/h$ Mpc.

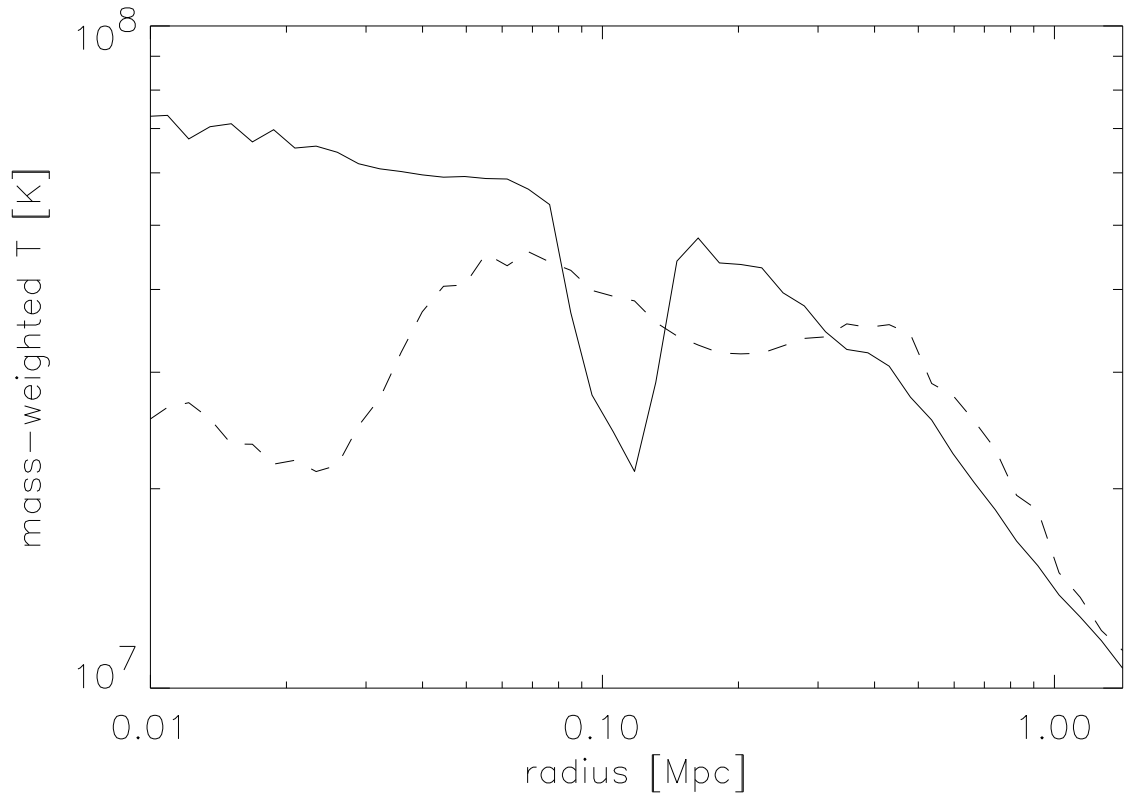


Fig. 2.— Mass-weighted temperature profiles for the most massive cluster in our simulation (see table 1). The solid line corresponds to the run with viscosity, while the dotted line corresponds to the run without viscosity.

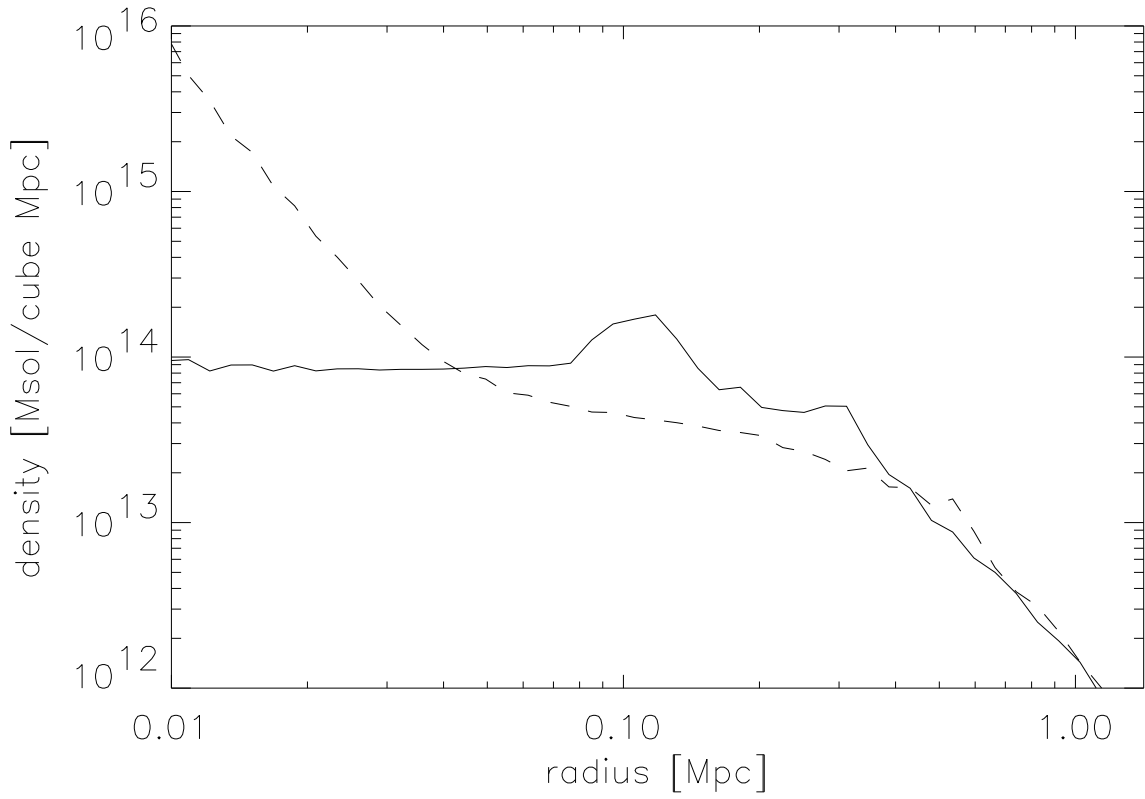


Fig. 3.— Density profiles for the most massive cluster. The units are $M_{\odot}/\text{Mpc}^{-3}$. The solid line corresponds to the run with viscosity, while the dotted line corresponds to the run without viscosity.

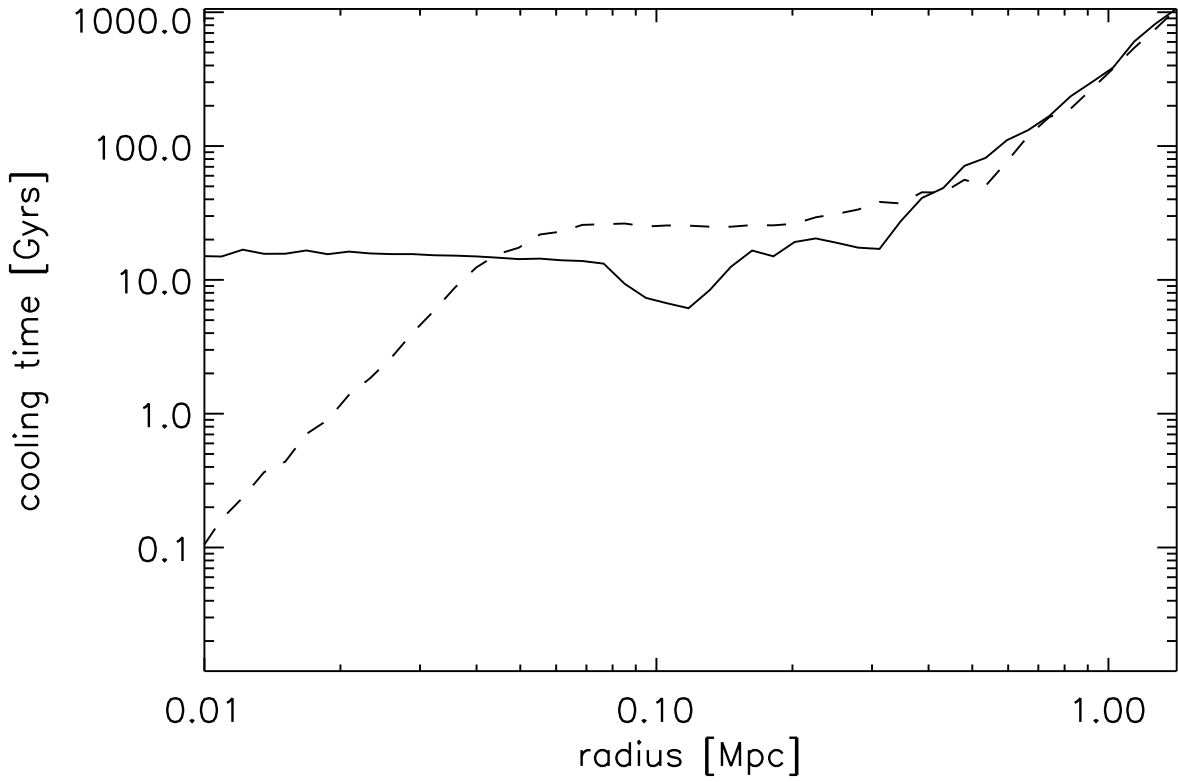


Fig. 4.— Cooling time (in Gyrs) profiles for the most massive cluster. The solid line corresponds to the run with viscosity, while the dotted line corresponds to the run without viscosity.

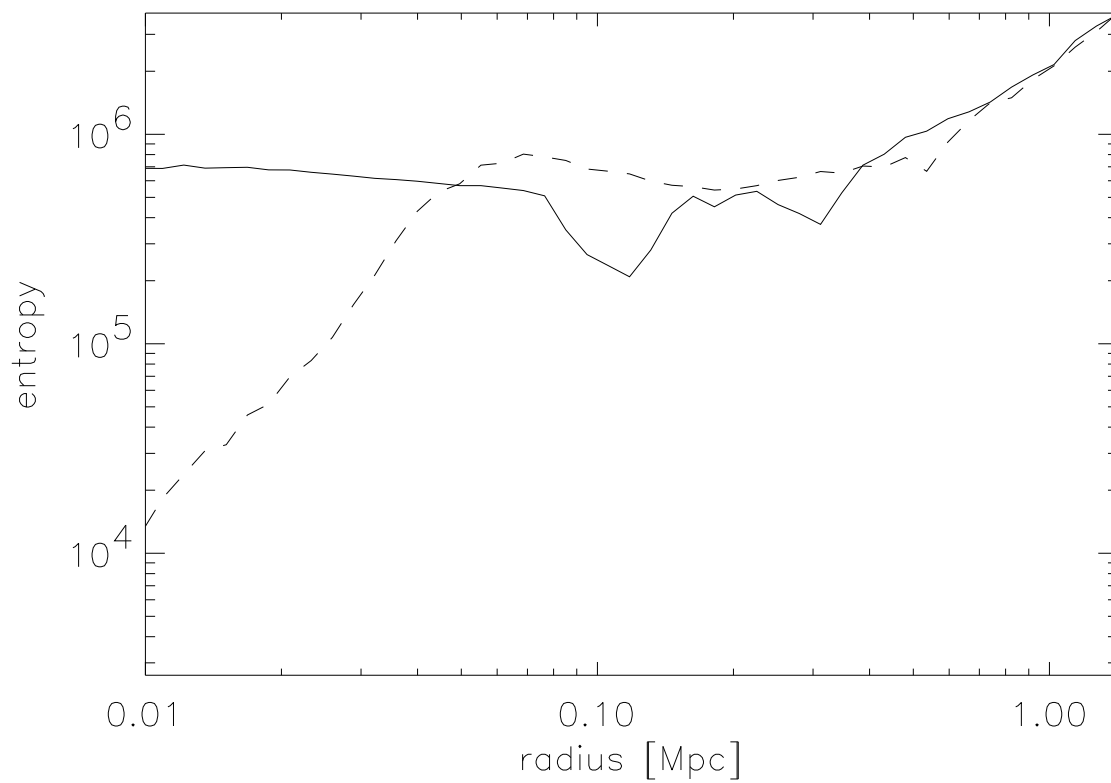


Fig. 5.— Entropy profiles for the most massive cluster. The solid line corresponds to the run with viscosity, while the dotted line corresponds to the run without viscosity.

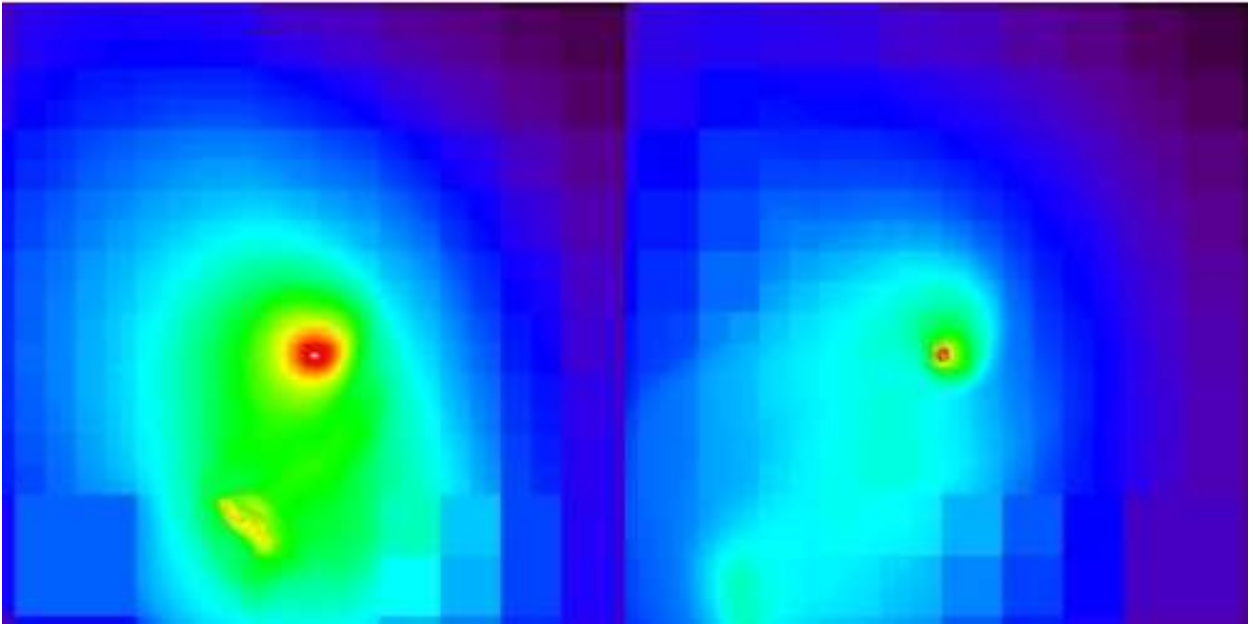


Fig. 6.— X-ray flux of the most massive cluster normalised to the maximum. The left panel shows the cluster simulated with viscosity. The right panel shows the cluster simulated without viscosity.

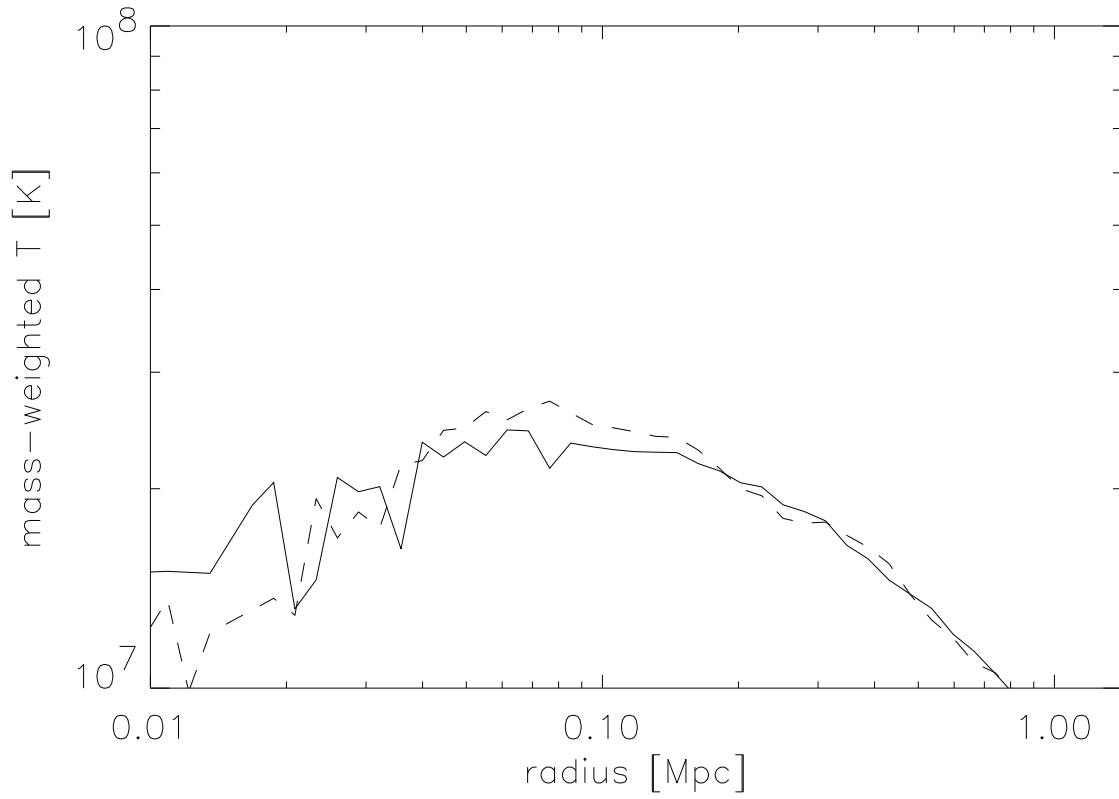


Fig. 7.— Mass-weighted temperature profiles for a smaller cluster with a mass of $9.7 \times 10^{13} M_{\odot}$. The solid line corresponds to the run with viscosity, while the dotted line corresponds to the run without viscosity.

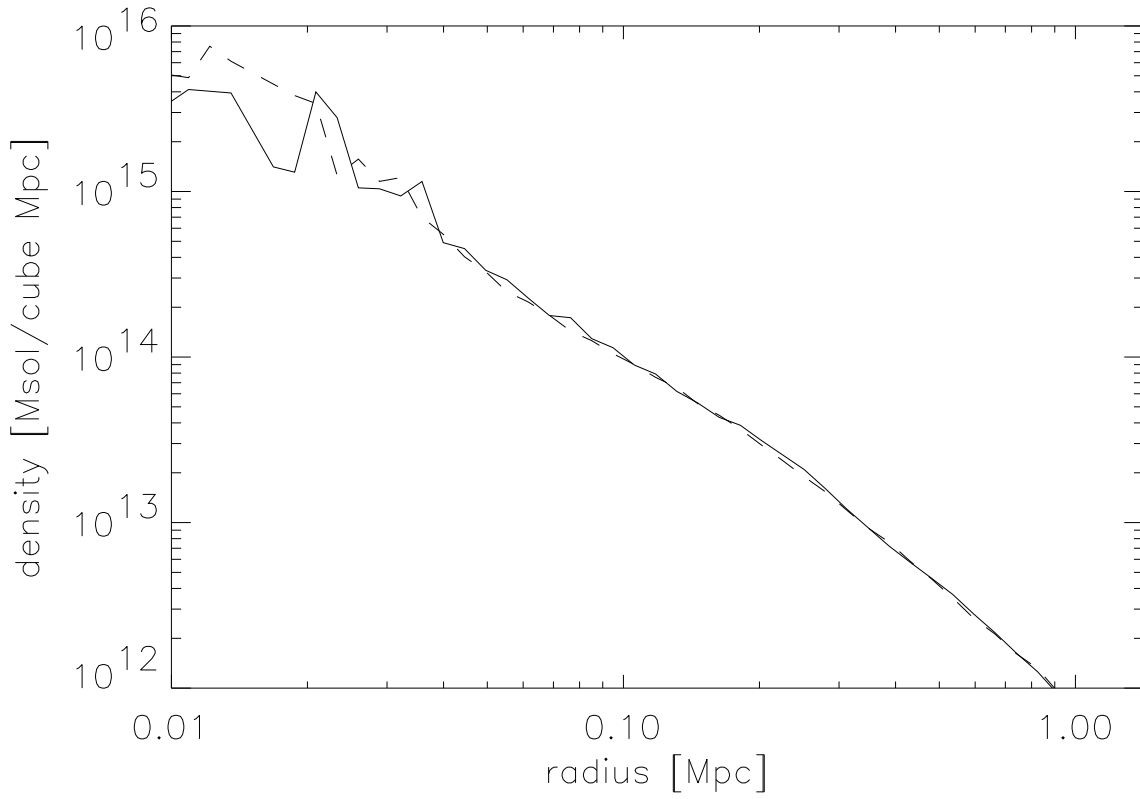


Fig. 8.— Density profiles for a smaller cluster with a mass of $9.7 \times 10^{13} M_{\odot}$. The units are $M_{\odot}/\text{Mpc}^{-3}$. The solid line corresponds to the run with viscosity, while the dotted line corresponds to the run without viscosity.

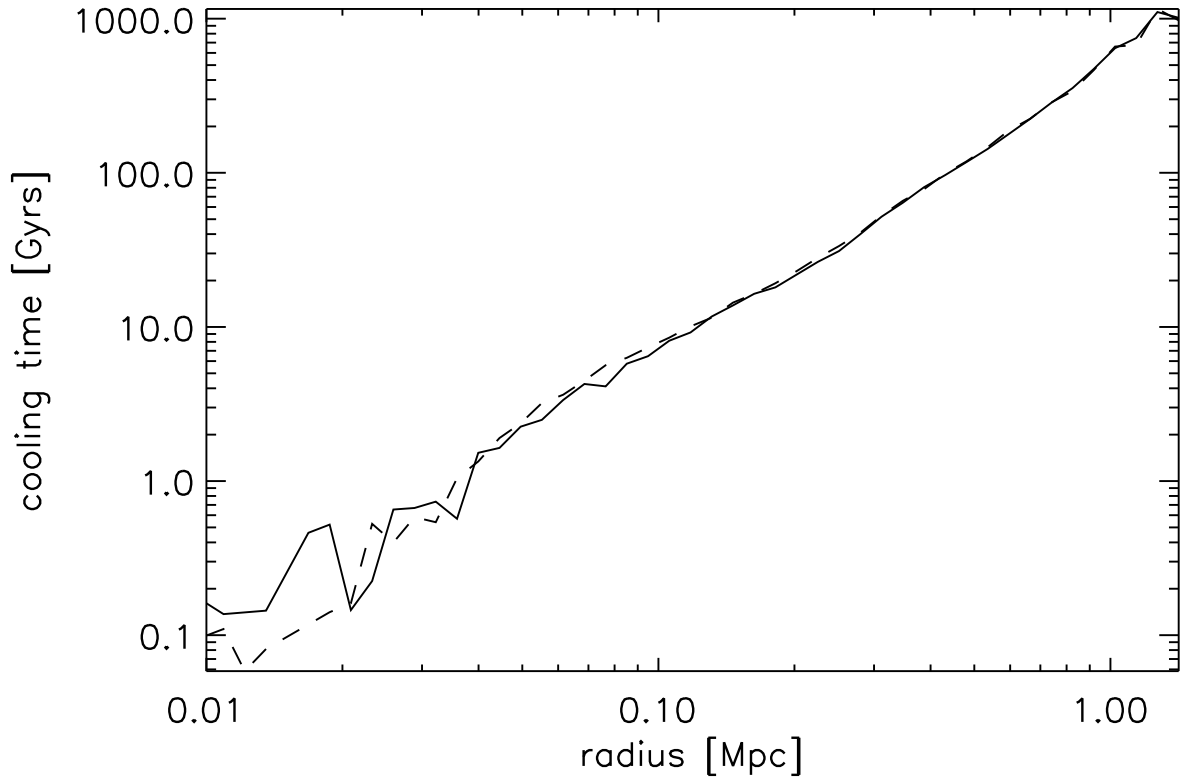


Fig. 9.— Cooling time (in Gyrs) profiles for a smaller cluster with a mass of $9.7 \times 10^{13} M_{\odot}$. The solid line corresponds to the run with viscosity, while the dotted line corresponds to the run without viscosity.